SANDIA REPORT

SAND98–1190
Unlimited Release
Printed June 1998

Experimental Results and Modeling of a Dynamic Hohlraum on SATURN

M. S. Derzon, G. O. Allshouse, C. Deeney, R. J. Leeper, T. J. Nash, W. Matuska, D. L. Peterson, J. J. MacFarlane, D. D. Ryutov

Prepared by
Sandia National Laboratories
Albuquerque, New Mexico 87185 and Livermore, California 94550

Sandia is a multiprogram laboratory operated by Sandia Corporation, a Lockheed Martin Company, for the United States Department of Energy under Contract DE-AC04-94AL85000.

Sandia National Laboratories

Issued by Sandia National Laboratories, operated for the United States Department of Energy by Sandia Corporation.

Printed in the United States of America. This report has been reproduced directly from the best available copy.

Available to DOE and DOE contractors from
Office of Scientific and Technical Information
P.O. Box 62
Oak Ridge, TN 37831

Prices available from (615) 576-8401, FTS 626-8401

Available to the public from
National Technical Information Service
U.S. Department of Commerce
5285 Port Royal Rd
Springfield, VA 22161

NTIS price codes
Printed copy: A03
Microfiche copy: A01

SAND98-1190
Unlimited Release
Printed June 1998

Experimental results and modeling of a dynamic hohlraum on SATURN

M. S. Derzon, G. O. Allshouse, C. Deeney, R. J. Leeper, T. J. Nash,
Pulsed Power Sciences
P.O. Box 5800
Sandia National Laboratories, Albuquerque, NM, 87185-1196

W. Matuska, D. L. Peterson, Los Alamos National Laboratory,

J.J. MacFarlane, University of Wisconsin - Madison

and D. D. Ryutov, Lawrence Livermore National Laboratory

ABSTRACT

Experiments were performed at SATURN, a high current z-pinch, to explore the feasibility of creating a hohlraum by imploding a tungsten wire array onto a low-density foam. Emission measurements in the 200-280 eV energy band were consistent with a 110-135 eV Planckian before the target shock heated, or stagnated, on-axis. Peak pinch radiation temperatures of nominally 160 eV were obtained. Measured early time x-ray emission histories and temperature estimates agree well with modeled performance in the 200-280 eV band using a 2D radiation magneto-hydrodynamics code. However, significant differences are observed in comparisons of the x-ray images and 2D simulations.

Acknowledgments

This paper shows the status of present state-of-the-art understanding and modeling of dynamic hohlraums in z-pinches; we thank Richard Bowers and Jack Brownell of LANL, Jim Hammer and Art Toor of LLNL for numerous discussions of this topic. We also thank Rick Spielman, Keith Matzen, Johann Seaman, Tom Sanford and others who learned how to increase the power on Saturn and for many technical discussions that helped guide us. We also thank the personnel at the Saturn facility and those responsible for the recent improvements in pinch performance for their assistance and support. Many thanks to Larry Hrubesh, John Poco, Hedley Lewis and A. Demiris of Lawrence Livermore National Laboratory for fabricating the foam targets and T. Gilliland of K-tech Corp. for their installation. L.P. Mix assisted with the image processing, and many useful discussions occurred with G.A. Chandler, T. Haill, E.J. McGuire, and M.A. Sweeney, of Sandia. This work was supported by the U.S. Department of Energy at Sandia National Laboratories under Contract No. DE-AC04-94AL85000. Sandia is a multiprogram laboratory operated by Sandia Corporation, a Lockheed Martin Company, for the U.S. Department of Energy.

At Sandia National Laboratories, we are studying the feasibility of creating a hohlraum[1,2] environment inside a magnetically imploded liner or z-pinch.[3,4,5,6,7,8,9] The hohlraum may be used to create an environment for the study of hot, dense matter[10] and inertial confinement fusion as well as other applications[11].

Most of the applications for these intense radiation sources require a radiation field decoupled from a shock. In particular, some z-pinch-based fusion concepts[12] have a fuel-containing capsule embedded in the pinch. A spherically symmetric radiation field is necessary to implode the capsule and fuel to the high densities and temperature required for fusion. In these pinch schemes the capsule implosion must occur before the arrival of a cylindrical shock due, to the imploding liner, at the capsule. For this reason, we quote the temperature at the shock arrival on-axis as an important figure-of-merit.

We report on the comparison of our experimental results with simulations of a 0.45 mg/cm tungsten liner imploded onto a 4-mm-diameter core of 0.9 mg/cm SiO_2 aerogel.[13,14,15] Fig. 1 is a schematic diagram of the target used in the experiment. In this experiment a cylindrical plasma formed from a tungsten wire array accelerated until striking the foam core, heating both the tungsten and the foam as well as generating a radiation wave and shock in the foam. The tungsten's' inertia and the magnetic field continue to compress the foam until the total mass assembles or stagnates on-axis. The imploding wire array was

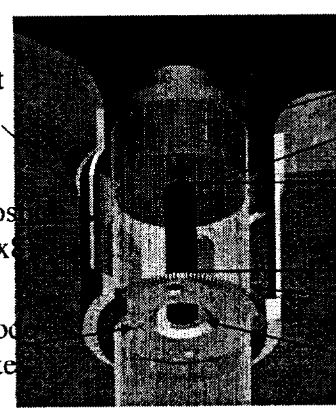

Fig. 1. Schematic of wire array z-pinch target with foam center.

120 tungsten wires 5 μm in diameter, arranged into a 17.5-mm-diameter, 2-cm-tall wire array of mass 0.45 mg/cm. The central foam core was a 4-mm-diameter SiO_2 aerogel of 7mg/cc, 2 cm long.

There was a 6-mm-diameter hole in the anode plate for on-axis measurements of the emission from the target and eight 6 mm wide slots in the current return can for viewing the target from the side. The side-on diagnostics view ~12 mm of the target height from a 35° angle to the horizontal, similar to the view shown in Fig. 1.

The dynamics of the pinch can be described as an initiation phase where joule heating creates a current carrying plasma sheath, followed by a run-in phase where the wire array is accelerated inward. These occur at early times, before 75 ns on Fig. 2. They are followed by what we call the strike, where the tungsten first impacts on the foam core. The late time sequence of events in the implosion of a wire onto foam is illustrated in Fig. 2, where the time history of the soft-filtered (200-280 eV) off-axis x-ray diode (XRD) signal is shown. Subsequent to the strike there is another run-

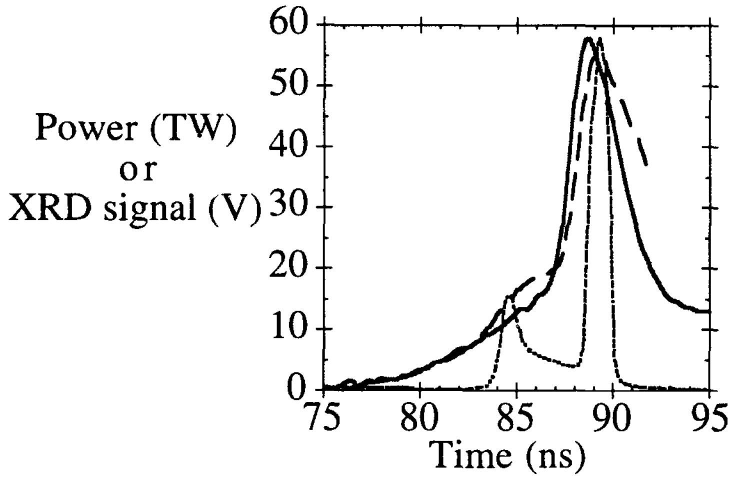

Fig. 2. XRD traces and X-ray emitted power. The solid trace is the measured Kimfol (200-280 eV) XRD output. The dotted curve is the calculated XRD voltage using 1D LASNEX normalized to the experimental data. The dashed line is the 3T diffusion estimate (2-D RMHD) of the calculated power-radiated.

in phase where a radiation wave and shock propagate through the foam to the axis until stagnation, when the current carrying sheath reaches the axis. The radiation wave and shock should precede the stagnation. Stagnation occurs as the tungsten-foam assembly ceases imploding and most of the remaining pinch kinetic energy is converted to thermal energy.

Radiated power is shown as calculated with a 1-D radiation magneto-hydrodynamics (1-D RMHD) code, LASNEX, with multigroup radiation transport[16] and a 2-D RMHD code simulation with three temperature (3T) radiation transport[17] (separate ion, electron and radiation temperatures). The 2-D modeling included the effects of magnetically driven Rayleigh-Taylor instabilities and the modeling has been compared to experiment with aluminum and tungsten wire arrays without the central foam targets.[18] The 1-D RMHD calculation shows two distinct peaks, whereas the experiment and 2-D calculations do not. The 1D calculations do not capture the either the radiation emission or the collision and deposition of energy in the strike; this is because the energy exchange times and transport times are short. Until the reasons for these differences are understood and accounted for 1D LASNEX should not be considered a credible tool modeling this class of experiments and perhaps no 1D model can.

A bolometer[19] measured the total radiation from the side of the pinch to be 400 $\pm$ 60 kJ; this compares with the calculated value of 450 kJ from the 2-D RMHD model. Within the differences generated using the different atomic physics and radiation transport models, the emission calculated agrees with the experimental result.

In this experiment, we studied the characteristics of the tungsten striking the foam by observation of soft x-ray (carbon-filtered) framing camera images.[20] The images are a complicated folding of the density, temperature, and opacity of the emitting material. In Fig. 3, we show soft x-ray images from the outside of the tungsten for wire arrays with and without a foam central cylinder. In the case without foam, there is a line

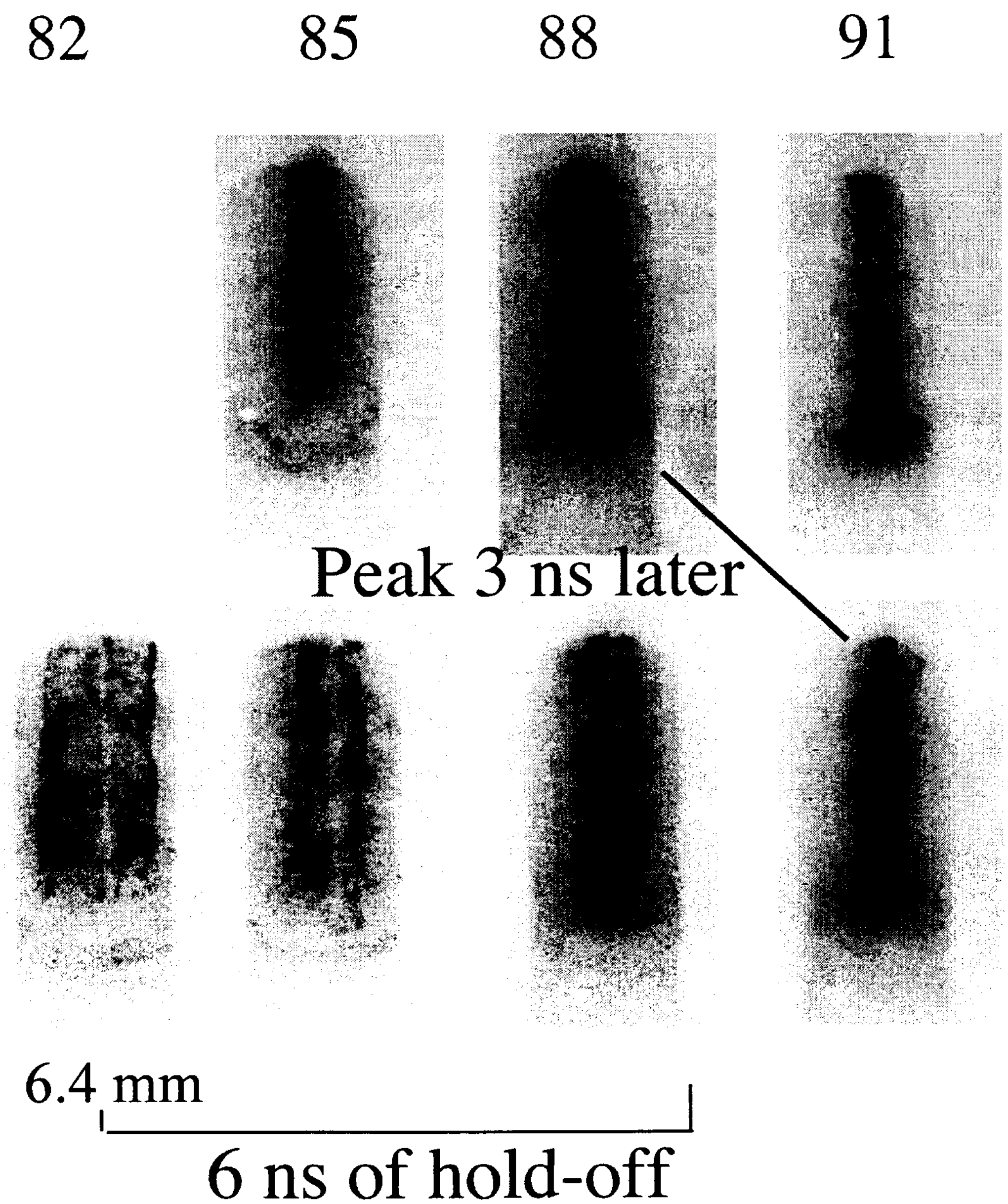

Fig. 3. Soft x-ray (200-280 eV) framing camera images of pinches without (top) and with (bottom) the central foam. The time in ns, with respect to figure 1, is shown above the images.

pinch that peaks in intensity at roughly 88 ns and exhibits a full width at half-maximum (FWHM) of ~ 1 mm. In the image with foam, at 82 ns a radiating shell is observed ~3 ns earlier than the peak in the case when no foam was present and the peak emission was delayed ~3 ns. The timing is consistent with the expected impact of the tungsten onto the foam core. The tightest pinch with foam occurs at ~ 91 ns with FWHM = 0.5 $\pm$0.2 mm; this is consistent with the slower velocity expected from the accretion of mass as the tungsten impacts the foam. The ~8 ns between the initial radiation from the strike to the rapid rise in emission, obtained from XRD data is evidence for the foam holding off the tungsten and creating a radiating shell; this is the process that would result in a hohlraum, or radiation confining, environment inside an imploding plasma shell. The emission in Fig.3 indicates 3D features in the non-uniformities, along both the z- and r-axis. The periodicities may also reflect instabilities. Rayleigh-Taylor and m=0 magneto-hydrodynamic instabilities may be observed in this data and have been discussed extensively in the literature. To put the observed intensity contrast in perspective, the roughly 30% variations observed reflect an approximately 7% variation in temperature if a Planckian source is assumed. Uniformity may be improved with more uniform central cylinders, this one was known to have axial and azimuthal variations in density. Another potential source of non-uniformities could be the 8-fold symmetry imposed on the magnetic field by the diagnostic slots in the current return can (see Fig. 1). These non-uniformities are being studied intensively.

In Fig. 4 we show an image generated by applying the transport equation and the T4 multigroup opacity library[21] to the calculated 2-D temperature and density structures[22,23]. This image is compared to the experimentally obtained image; both are at 85 ns. The rings in the intensity of the simulated image are due to the calculated Rayleigh-Taylor instability growth. Although not obvious in the reproduced image, there are faint ring structures in the data reflecting this effect. The rings in both the calculations and data have roughly the same spatial frequency (~4/cm along the z-axis) based on intensity fluctuations. In the modeling, the rings are due to high temperature regions that occur at the tungsten/SiO_2 foam interface that are at significantly higher temperature than the surrounding 'bulk' plasma. The spatial extent (not frequency) of the features is of mm scale in the data and ~100 μm in calculations. One potential explanation for this is that the cell size is 100 μm in the calculation and higher resolution is required, however, with present resources higher resolution modeling is not practical. Another potential explanation is that inherently 3D effects broaden these features.

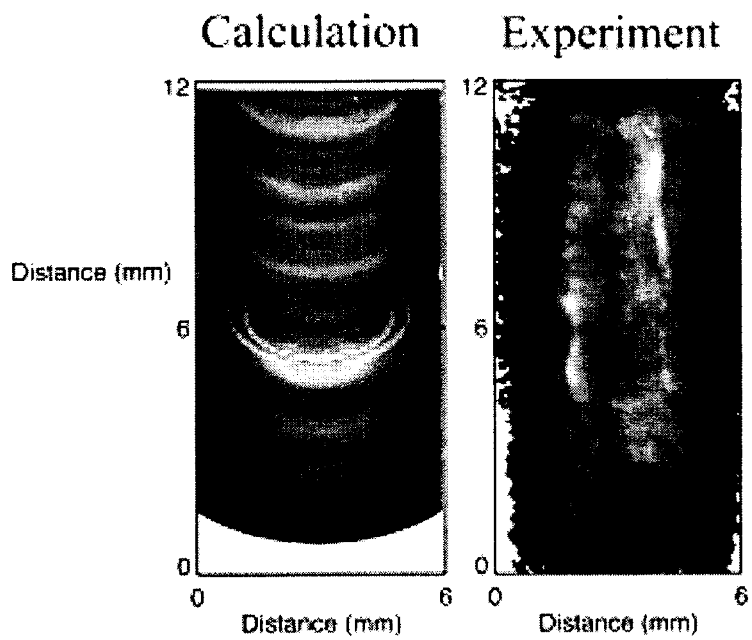

Fig. 4. Simulated soft x-ray framing-camera image and data at 85 ns.

In addition, the data shows low intensity along the z-axis, and small intense regions in the r-domain at large r, ~1.5 mm (see Fig. 4) that are not in the simulated image. These effects are quantified in Fig. 5, where lineouts were taken through the images. These lineouts show the radial variations in intensity. The main feature size is larger than the 4 mm initial foam diameter because of ablation of the inner target. The wire array plasma maintains a ~30 eV temperature according to the calculation which heats and ablates the inner foam target due to Joule heating. The high spatial frequency feature in r, at the target edge, is not reproduced in the modeling at these times; it does appear at earlier times.

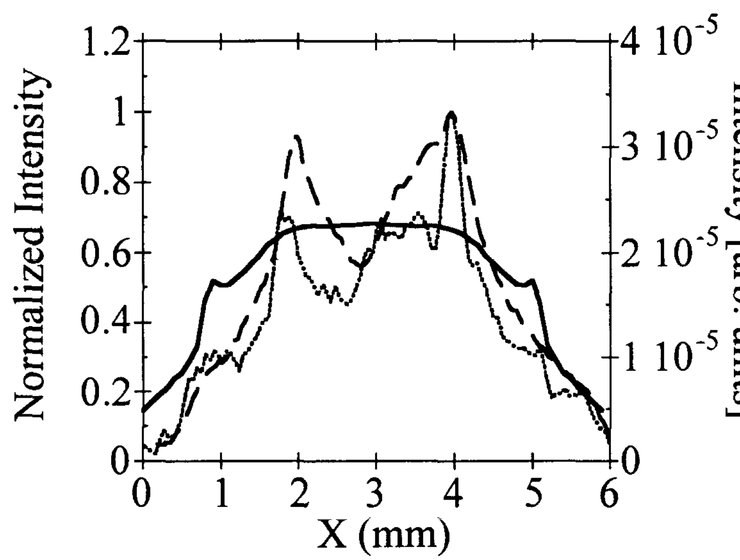

Fig. 5. Comparison of emission profiles for radial lineouts of the 85 ns framing camera image. Δy ~ 1mm (dotted trace), and Δy ~ 5 mm (dashed trace) compare the experimental result to the to calculated profile at 85 ns with the modeled image for Δy = 5 mm (solid curve).

A possible explanation for the decrease in intensity along the axis is the optical closure of the slot due to material ablating from the current return can; this is a concern and an active area of investigation. However, it is not believed to be the cause of the feature because it is not observed in the shots without foam and there is evidence that 4 mm diameter diagnostic holes do not close. In summary, although the emission history as calculated (2D) agrees with the measured result, the simulations do not capture all of the important features of the radiation production.

There are a number of reasons that the modeling may not be capturing the physics apparent in the data images. There are inherent limitations in the diffusion model, or 3D effects related to the magnetic fields or instability growth could be important. There is also evidence that the large spike and bubble density variations obtained in the calculations may be an artifact of the averaging algorithms used to determine zone properties. These are all being studied.

The temperature of the hohlraum is considered the most important figure-of-merit. Temperature estimates have been made by folding the emission history into the source size. This resulted in area-averaged brightness temperatures. They were obtained from calibrated bandpass filtered x-ray diodes[24] (XRDs) that provided source brightness for broadband (dE/E~0.3) spectral regimes. The size, FWHM, of the emitting region was obtained from the framing camera images and fitted to a quadratic in time. The quadratic is a good fit to the data until roughly 90 ns. An important caveat in interpreting the size data is that the cameras measure the size from the side, not the end. The emission spot is expected to be smaller end-on, which would result in higher temperatures. We assumed a uniform Planckian (<8% effect), Lambertian source of this size and unfolded a brightness temperature based on the calculated sensitivity of the XRD's. This was done for XRD's located on axis and at the 35° location. Quoted uncertainties include detector and filter effects on sensitivity but not the effect of non-uniform emission.

In Fig. 6. we show an important comparison. The brightness temperature for the 200-280 eV XRD channel is compared to the calculated mean electron temperature in the aerogel from the 2D. This is an important comparison for it most closely represents the energy transferred to the foam as a function of time, and the radiation out the end of the target, which we measure. In the calculation, stagnation begins at roughly 87 ns consistent with an internal temperature of 110 eV, 135 eV from the fitted data. Until peak temperature there is agreement between the measured and calculated temperatures inside the wire array suggesting that the energy densities and balances are acceptably calculated. Internal foam temperatures were 25 $\pm$ 7 eV higher than the outer surface of the tungsten[15] before the target stagnation feature. The combination of high internal temperature and the gradient in temperature to the edge of the tungsten implies that the tungsten is acting as a case to confine the energy, i.e. as a hohlraum.

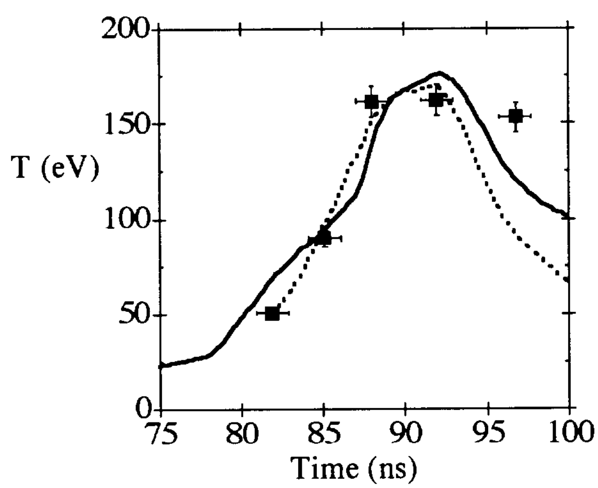

Fig. 6. a) Brightness temperature obtained on-axis and calculated, 2-D RMHD, electron temperature in the foam (solid line). Square points are the data using the size from the framing camera. Dashed line was generated using the size from a quadratic fit to the first four frames of the framing camera.

A problem with unfolding a temperature in this way is that the source is non-uniform. The source is known to be non-Planckian. This is in the sense that there is less high energy content in the spectrum than is calculated or would be present with a Planckian source (based on unfolding higher energy channel detectors, and not discussed in this paper). There are additional interpretive difficulties created by using an area-averaged temperature of a system with known temperature variations, particularly when the source is not opaque. These include aperture closure, tungsten blowing through the aperture, jetting of low-density plasma along the axis, and non-uniformities in the source. Analytic estimates of each of these have been made; the jet is expected to keep the aperture open and to remain optically thin. The non-uniformities are of concern and plans are being made to diagnose the end-on emission field.

In summary, time-resolved brightness temperature estimates were made of the foam central cylinder and compared to a detailed 2-D RMHD simulation. Calculated 2-D emission histories agree well ($\pm$ 10% in temperature) with the experiments. From the rough agreement in the waveforms of Fig. 6, prior to 92 ns, we conclude the overall energy balance is modeled fairly well. However, details of the radiation emission are not all captured correctly in the modeling based on the image analysis. These results described are consistent with a dynamic (imploding) z-pinch hohlraum; they show the current state of our understanding and highlight critical area requiring further study.

References

[1] -J. Lindl, Physics of Plasmas, **2**, No. 11, 1(1995)

[2] -M.S. Derzon, et al, Phys. Rev. Lett., **76**, No. 3, 435(1996)

[3] -N.R. Periera and J. Davis, J. Appl. Phys., 64, No. 3(1988)

[4] -J. H. Brownell and R. L. Bowers, "The flying radiation case', Bull. of the 37th meeting of the APS-DPP Nov. (1995), NIST #DE-97004733, LANL Report LA-UR-97-558, 1997

[5] - M. S. Derzon, Rev. Sci. Instr., **68**, No. 1, 848(1997)

[6] - D.L. Peterson, R.L. Bowers, J.H. Brownell, A.E. Greene, K.D. McLenithan, T. A. Oliphant, N.F. Roderick, and A.J. Scannapieco, Phys. Plasmas **3**, 368(1996)

[7] - M.K. Matzen, Phys. Plas. **4**, No. 5, 1519(1997)

[8] - D.D. Ryutov, submitted to Reviews of Modern Physics, 'The Physics of Fast Z-Pinches'

[9] - C. Deeney, et al., Phys. Rev. E, **56**,No. 5(1997), to be published

[10] - Dept. of Energy 5 year plan. PLL directive. January 1997.

[11] - J. Porter, et al., Bull. of the 37th meeting of the APS-DPP Nov. (1995)

[12] - R.E. Olson, et al, Phys. Plasmas **4**, (5), 1818(1997)

[13] - Fabricated by L. Hrubesh, Lawrence Livermore National Laboratory

[14] - Characterization of a sample of this aerogel foam by ion microtomography is described in Antolak, A., Rev. Sci. Instr., **68**, No. 1, 858(1997)

[15] - T.J. Nash, et al., 'Dynamic Hohlraum Experiments on SATURN', submitted to the 1997 4th Intern. Conf. on Dense Z-pinches, May 28-30, Vancouver, Canada, ed. N. Periera and J. Davis to be published by the Amer. Inst. Phys.

[16] - G. B. Zimmerman and W.L. Kruer, Comments on Plasma Phys. Controlled Thermo. Fusion **2**, 51(1975)

[17] - D.L. Peterson, R.L. Bowers, J.H. Brownell, A.E. Greene, K.D. McLenithan, T.A. Oliphant, N.F. Roderick, and A.J. Scannapieco, Phys. Plas. **3**, (1), 386(1996)

[18] - D.L. Peterson, R.L. Bowers, J.H. Brownell, C. Lund, W. Matuska, K. McLenithan, H. Oona, C. Deeney, M. Derzon, R.B. Spielman, T. J. Nash, G. Chandler, R.C. Mock, T.W.L. Sanford, M.K. Matzen, N.F. Roderick, 'Application of 2-D Simulations to Hollow Z-Pinch Implosions', Invited paper, submitted to the 1997 4th Intern. Conf. on Dense Z-pinches, May 28-30, Vancouver, Canada, ed. N. Periera and J. Davis to be published by the Amer. Inst. Phys.

[19] - D.L. Hansen, 'User guide to the SNL Bolometer:A Time resolved diagnostic for soft x-ray energy measurements', Febuary 8, 1984, internal memo.

[20] - The camera used had nominally a 100-ps gate, a 3-ns interframe time and 70-200 μm resolution.

[21] - J. Abdallah, and R.E.H. Clark, 'TOPS: A multigroup Opacity Code', LA-10454

[22] Matuska, W., J. Benage, G. Idzorek, C. Lebeda, D Peterson, Proc. of the 1995 IEEE International Pulsed Power Conf., Alb. NM, 1995

[23] - Matuska, W., R.L. Bowers, J.H. Brownell, H. Lee, C.M.Lund, D.L. Peterson, and N.F. Roderick, Phys. Plasma **3**,1415(1996)

[24] - D.L. Fehl, G.A. Chandler, F. Biggs, R.J. Dukart, A.R. Moats, and R.J. Leeper, Rev. Sci. Instr., **68**, No. 1, 843(1997)

Sand Report Distribution –

'Experimental results and modeling of a dynamic hohlraum on SATURN'

Sandia National Laboratory

#	name	Org.	MS
1	Bailey, James E.		1186
1	Chandler, Gordon		1196
5	Cook, Don	9500	1190
1	Cuneo, Michael	9533	1186
5	Deeney, C.	9573	1194
1	Desjarlais, M.	9533	1186
10	Derzon, M.S.	9577	1196
1	Douglas, M.	9574	1194
1	Fehl, David	9577	1196
1	Haill, Tom	9574	1187
1	Hamil, Roy	9512	1188
1	Kiefer, Mark	9542	1186
1	Lash, J.	9574	1187
10	Leeper, Ray	9577	1196
1	Maenchen, John	9515	1193
1	Marder, B.	9574	1187
5	Matzen, Keith	9570	1187
1	McDaniel Dillon	9573	1194
1	McGuire, Eugene	9574	1187
1	Mehlhorn, T.	9574	1186
1	Moats, Anne	9577	1196
5	Nash, Tom	9577	1196
1	Olson, Craig	9500	1188
1	Olson, Richard	9577	1187
5	Quintenz, Jeffrey	9502	1191
1	Ramirez, Juan J.	9580	1178
1	Rochau, G.A.	9580	0741
1	Rochau, G.E.	9580	1196
1	Rosenthal, S.	9544	1186
1	Ruiz, Carlos	9577	1196
1	Slutz, Stephen	9574	1186
1	Spielman, Rick	9573	1194
1	Stygar, William	9573	1194
1	Sweeney, M.A.	9502	1186
1	Yonas, G.	9000	0151

----

1 Central Tech. Files 8940-2, MS-9018

5 Technical Library 4916, MS-0899

2 Review and Approval Desk, Org. 12690, for DOE/OSTI, MS-0619

5 Lawrence Livermore National Laboratory
Att: D.D. Ryutov, L-630
Livermore, CA 94551

5 Los Alamos National Laboratory
Att: D.L.Peterson, B-259
Los Alamos, NM, 87545

5 Los Alamos National Laboratory
Att: W. Matuska, B-259
Los Alamos, NM, 87545

5 J.J. MacFarlane
Fusion Technology Institute
1500 Engineering Dr.
UW-Madison, 53706

1 Los Alamos National Laboratory
Att: R. Bowers, B-259
Los Alamos, NM, 87545

1 Los Alamos National Laboratory
Att: M. Jones, B-259
Los Alamos, NM, 87545

1 Los Alamos National Laboratory
Att: J. Aubrey, B-220
Los Alamos, NM, 87545

1 Lawrence Livermore National Laboratory
Att: A. Toor, L-041
Livermore, CA 94551

1 Lawrence Livermore National Laboratory
Att: J. Hammer, L-477
Livermore, CA 94551